Image-based Ear Biometric Smartphone App for Patient Identification in Field Settings

Sarah Adel Bargal[1], Alexander Welles[2], Cliff R. Chan[3], Samuel Howes[2], Stan Sclaroff[1], Elizabeth Ragan[4], Courtney Johnson[4] and Christopher Gill [4]

[1]*Computer Science Dept.,* [2]*Computer Engineering Dept.,* [3]*Electrical Engineering Dept.,* [4]*School of Public Health*

Boston University, Boston, MA, USA

{*sbargal, awelles, crchan, showes, sclaroff, ejragan, courtj, cgill*}*@bu.edu*

Keywords: Smartphone, Application, Public Health, Biometrics

Abstract: We present a work in progress of a computer vision application that would directly impact the delivery of healthcare in underdeveloped countries. We describe the development of an image-based smartphone application prototype for ear biometrics. The application targets the public health problem of managing medical records at on-site medical clinics in less developed countries where many individuals do not hold IDs. The domain presents challenges for an ear biometric system, including varying scale, rotation, and illumination. It was not clear which feature descriptors would work best for the application, so a comparative study of three ear biometric extraction techniques was performed, one of which was used to develop an iOS application prototype to establish the identity of an individual using a smartphone camera image. A pilot study was then conducted on the developed application to test feasibility in naturalistic settings.

1 INTRODUCTION

Tracking medical data in regions where conventional forms of patient identification are lacking or poorly maintained can pose unique challenges for medical professionals. For example, in less developed countries, ID numbers may not be present and address and name spellings may be inconsistent. When patient identity cannot be reliably determined, undesired consequences such as treatment duplication and disruption of longitudinal patient care may occur.

Biometrics can be used for tracking identity in the global health application scenario. Fingerprinting, facial recognition, iris scanning, and palm-printing are not optimally suited for this application domain. If fingerprints are used to identify patients, then this may discourage individuals from seeking medical care due to the widespread use of fingerprinting in law enforcement. Facial recognition raises privacy concerns: in [Azfar et al., 2011], 58% of 89 HIV patients said that face photography is acceptable for teledermatology care, whereas acceptability is above 90% for photography of other body parts. Iris scanning requires user cooperation in viewing iris reflection [Delac and Grgic, 2004]; this can be difficult for children. Palm printing and fingerprinting raise hygiene issues due to many people touching the same surface.

In this work we use ear biometrics. Ears can be photographed without an invasive or uncomfortable procedure. The image capture process is contactless, and therefore no hygiene problems arise. Photographing the ear is not associated with the stigmatizing effects of photographing the face or taking fingerprints. Ear shape does not change significantly with age (after the first two to three years of life) [Iannarelli, 1989].

In this paper we conduct a work in progress for a smartphone application (app) that can easily be used by a field health worker seeing many patients on a daily basis. Smartphones are cheap and deployable in different field settings. Figure 1 shows the envisioned use case scenario of the target application. On an initial patient visit, one or more images of an individual patient's ear are captured. Ear descriptors are extracted and stored in a database along with basic patient information. On another visit, responsible personnel capture an image of the patient's ear. Database records that possibly match are retrieved in the form of a ranked list.

Recognition rates are highly dependent on: locating the ear in the captured image, and matching ears captured at different angles, scales, and illumination conditions. The more resilient a system is to these factors the better it may perform. In developing

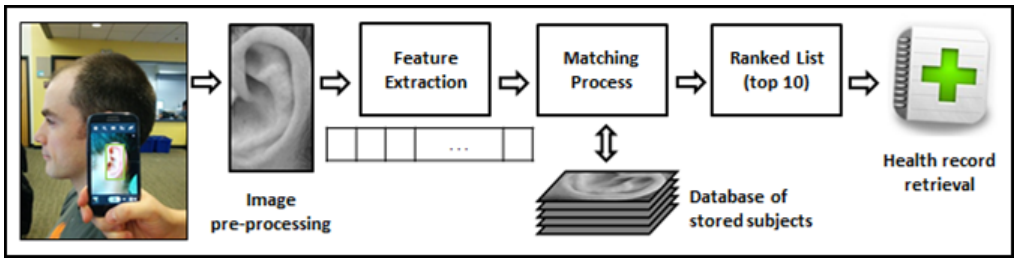

Figure 1: System diagram of the proposed smartphone app for patient identification in field settings.

our system, we tested and compared three commonly used feature extraction techniques that each address at least two of these challenges by design: Local Binary Patterns (LBPs), Generic Fourier Descriptor (GFD), and Scale Invariant Feature Transform (SIFT). These were validated on a controlled dataset of 493 images of 125 individuals. We then used SIFT to develop an iOS app prototype as a proof of concept. A pilot study was then conducted on the app using a dataset of 838 images of 240 individuals.

2 RELATED WORK

The advancement of onboard sensors is allowing for biometric identification, in smartphones. In [Kwapisz et al., 2010] accelerometry is used to identify and authenticate an individual based on their movement signatures in daily behavior. This is useful in personal devices only. Descartes Biometrics developed the 'Ergo' system that uses the smartphone touch screen sensor to identify a user by an ear print in combination with movement signatures of how the phone is picked up [Goode, 2014]. Pressing patients' ears against a touch screen could raise hygiene problems in the field.

In [Fahmi et al., 2012], a feature extraction technique based on ear biometrics is proposed, and authors predict that it would be directly applicable on a smartphone. In [Kumar, 2014], the following idea is mentioned: allowing parents or health care workers to take ear and feet images of a child and send them to a central server that sends back a text message with the vaccination needs. This idea assumes the availability of a smartphone with the parent, and the availability of a running network to a central server. Such assumptions may not hold in the underdeveloped field settings we target. This also assumes that the top match will be the correct one 100% of the time. Both [Fahmi et al., 2012, Kumar, 2014] do not report working implementations or quantitative results. Before smartphone applications for biometrics, there has been a wealth of research performed in automating the various subtasks of an ear detection

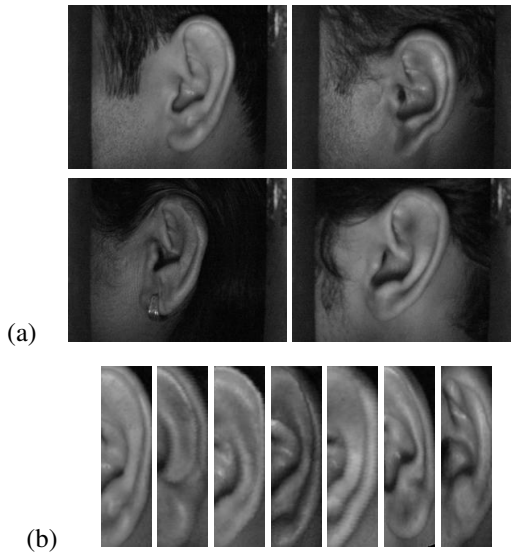

Figure 2: Sample ear images from the IIT Delhi Ear Image Database [Biometrics Research Laboratory, 2013], (a) raw (b) pre-processed.

system [Abaza et al., 2013]. Various approaches use a three-dimensional or two-dimensional ear representation. $2D$ approaches are more appropriate for our domain because of the field requirements of fast and cheap solutions. Extracting a feature vector from a $2D$ ear representation has been done in many ways including Eigen Ears (PCA) [Chang et al., 2003], Force Field [Abdel-Mottaleb and Zhou, 2005], GFD [Abate et al., 2006], SIFT/SURF [Cummings et al., 2010, Kisku et al., 2009], and LBPs [Wang et al., 2008, Boodoo-Jahangeer and Baichoo, 2013].

3 COMPARATIVE STUDY: FEATURE EXTRACTION

In our application, potentially matching records are presented to the health worker, ranked in order of ear biometric similarity, given an image of an individual patient's ear. If a record of that individual is already

enrolled in the database then that individual's record should appear ranked in the first position (first nearest neighbor), or at least within the top 5 to 10 records (within 5 or 10 nearest neighbors).

With this use case in mind, we conducted a comparative evaluation of three widely used ear biometric feature representations: Local Binary Patterns (LPBs), Generic Fourier Descriptor (GFD), and Scale Invariant Feature Transform(SIFT). These experiments were conducted using the IIT Delhi Ear Image Database [Kumar and Wu, 2012], which contains 493 images of 125 subjects whose ages range between 14 and 58 years. The number of images per individual in the dataset varies between 3 and 6. The camera was partially covered from the side so that direct light from indoor illumination does not enter the camera. Original captured images have a resolution of 272×204 pixels, but the dataset also offers automatically normalized and cropped ear images of 50×180 pixels. Sample images, raw and pre-processed, can be seen in Figure 2(a) and 2(b) respectively. In the rest of this section, we report our experimental setup for the comparison of the three approaches.

3.1 Local Binary Patterns

LBPs [Ojala et al., 1996] demonstrated good performance in ear biometrics [Wang et al., 2008, Boodoo-Jahangeer and Baichoo, 2013]. Following [Takala et al., 2005, Wang et al., 2008] we use P sampling points on a circular grid of radius R, and uniform binary patterns u2 originally introduced by [Mäenpää et al., 2000] ($LBP^{u2}_{(P,R)}$). Our implementation is based on the rotation invariant MATLAB implementation of Marko Heikkil and Timo Ahonen. In our work, we perform experiments on 54 LBP variants resulting from the Cartesian product of the following parameter settings:

- Images: We experimented with a) the full resolution image, b) the concatenation of the vertical, horizontal and diagonal images resulting from single-level 2D wavelet decomposition with respect to Daubechies of size 20 (empirically determined), and c) the blurred and subsampled image ($1/2$ each dimension).
- Regions: We experimented with partitioning an ear image into 1, 2, 3, 4, 6, and 8 regions as depicted in Figure 3.
- Neighborhoods and Radii: We experimented with neighborhood and radii sizes (8,1), (8,2), and (16,2).

The final dimensionality depends on the number of input images used, the number of regions, and the size of the neighborhood. The shortest feature vector was of length 10, and the longest was of length 432. Out of the 54 possible combinations of parameter settings, $LBP^{u2}_{(16,2)}$ with 6 regions and downsampling gave the best recognition rates. Then we explored concatenating (+) feature vectors of different neighborhoods to have a multi-scale descriptor, and $LBP^{u2}_{(8,1)} + LBP^{u2}_{(16,2)}$ with 6 regions and downsampling gave the highest recognition rates.

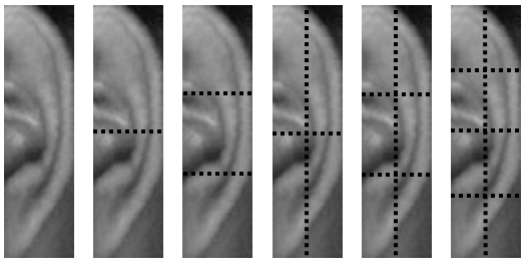

Figure 3: Different image divisions used for the LBP number of regions parameter.

3.2 Generic Fourier Descriptor

The Generic Fourier descriptor (GFD) proposed by [Zhang and Lu, 2002] was reported successful in ear biometrics [Abate et al., 2006]. GFD uses a modified polar Fourier transform (PFT) which makes it rotation invariant. The magnitudes of the resulting Fourier coefficients are stored in a vector and normalized as follows:

$$GFD = \left\{ \frac{|PFT(0,0)|}{Area}, \frac{|PFT(0,1)|}{|PFT(0,0)|}, \cdots, \frac{|PFT(R,T)|}{|PFT(0,0)|} \right\}. \quad (1)$$

The first magnitude value is divided by the circle's area. The remaining ones are normalized by the first magnitude (DC). By only keeping the magnitude of the Fourier coefficients, the GFD effectively becomes rotation invariant. Scale invariance can be obtained by initially placing the circle such that the top and bottom of the ear hit the perimeter, and then consistently sampling. This method is also illumination invariant due to the DC coefficient normalization over the average image brightness.

In our work, we used the same descriptor. We implemented PFT on a square input image, resized to 128×128 pixels (Figure 4). Empirically, we found that 64 radial and 180 angular samples yielded the best results.

When testing the GFD during classification, we noted that the inclusion of the first GFD value had a detrimental impact on the overall accuracy for our data set. The first GFD term represents the average

image brightness and is not feature descriptive. The removal of this term resulted in an overall increase in accuracy during testing.

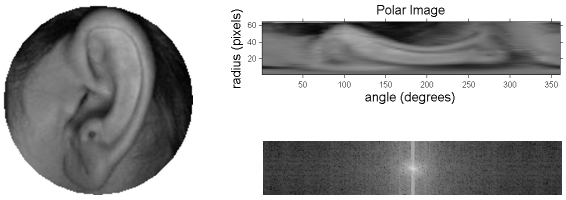

Figure 4: Example image with its corresponding polar image representation (top right), and corresponding Fourier spectrum (bottom right).

3.3 Scale Invariant Feature Transform

SIFT features [Lowe, 1999] have been successfully used in ear biometrics by [Cummings et al., 2010, Kisku et al., 2009]. SIFT features are scale and rotation invariant, and only show some illumination tolerance. In our work, we used the open source library vl_feat [Vedaldi and Fulkerson, 2008] for extracting and matching SIFT features in MATLAB, and the OpenCV SiftFeatureDetector function [Bradski, 2000] is used in C++ for the iOS application. The default parameter settings were used for vl_feat, but we empirically determined parameter values for the OpenCV SiftFeatureDetector for use on images captured by the camera of the smartphone device. The first parameter controls the number of best features to retain; we retain all features. The second parameter controls the number of Octave Layers. The number of octaves is computed automatically from the image resolution. The third parameter is a threshold that controls filtering out weak features in low-contrast regions. The fourth parameter is a threshold that controls filtering out edge-like features. The fifth parameter is the scaling parameter for the Gaussian Kernels used in SIFT's Gaussian pyramid for identifying potential keypoints. In our empirical study we determined that the following settings worked best: nfeatures=0 (default), nOctaveLayers=3 (default), contrastThreshold=0.025, edgeThreshold=20, sigma=1.0.

4 RESULTS: COMPARATIVE STUDY

Our biometric application is to retrieve a ranked list for an individual. We pose this as a k-Nearest Neighbor (k-NN) problem where the user will be presented with the top k matches. So we evaluated performance of LBPs, GFD, and SIFT on a k-NN retrieval task, first with $k = 1$ requiring the top match to be the correct one, then with a reasonable k size that a user can handle.

As the system is used, more image descriptors will be available. We are interested to see how the system performs as we train on more images. The IIT dataset contains at least 3 images per subject. We evaluated performance when the number of images per individual in the database was varied: 1 image per individual, 2 images, and n-1 images, where n is the total number of images available for that particular individual. 3-fold cross validation was conducted every time. In the rest of this section we report evaluation of the three approaches and provide a summary comparison.

4.1 Local Binary Patterns

To perform 1-NN retrieval with LBPs we tested different distance metrics: Euclidean, City Block, and Correlation, to compare their performance. The results are summarized in Table 1. The table reports the accuracy of retrieving the correct individual in the rank 1 position using the best performing LBP feature vector: $LBP^{u2}_{(16,2)}$ with 6 regions and downsampling.

As expected, we noted improvement in 1-NN retrieval as the number of training examples per individual increases. Overall, the best performing metric is City Block in the different testing rounds, but it is equivalent to Euclidean when we train on n-1 images, which is the steady state of our system.

For comparison, a Support Vector Machine (SVM) was used for classification. Experimentation was performed with different kernel functions: linear, quadratic, polynomial, and rbf (varying parameter values). A multi-class linear SVM performed best, but did not out-perform 1-NN as reported in Table 1.

After examining the results from this experiment, we experimented using multi-scale LBP and Euclidean distance 1-NN. This is conducted using the concatenation (+) of LBP feature vectors of different radii and neighborhoods. An improvement over the best feature vector in Table 1 is obtained by $LBP^{u2}_{(8,1)}$ + $LBP^{u2}_{(16,2)}$ with 6 regions and downsampling giving a recognition rate of 95.5%.

4.2 Generic Fourier Descriptor

To perform 1-NN retrieval with GFD, we tested different distance metrics: Euclidean, City Block, and Correlation, to compare their performance. The results are summarized in Table 2. The table reports

Table 1: Results using LBPs for feature extraction.

	# Images in Training Dataset		
	1	2	$n-1$
1-NN Euclidean	83.2%	91.7%	94.9%
1-NN City Block	87.3%	93.9%	94.9%
1-NN Correlation	81.5%	90.9%	93.3%
SVM	–	–	80.3%

the accuracy of retrieving the correct individual in the rank 1 position using the best performing polar sampling rate.

As with LBPs, the inclusion of more images (per individual) in the training database resulted in an increase in the accuracy for all distance measures. Euclidean and Correlation give marginally higher recognition percentages than City Block on n-1 images, which is the steady state of our system. Euclidean performs marginally better than Correlation when training on a single image.

Table 2: Results using GFD for feature extraction.

	# Images in Training Dataset		
	1	2	$n-1$
1-NN Euclidean	84.8%	94.4%	96.0%
1-NN City Block	84.9%	93.9%	95.2%
1-NN Correlation	84.5%	94.4%	96.0%

4.3 Scale Invariant Feature Transform

SIFT was used in 1-NN. Distances between matching SIFT keypoints were returned by vlfeat and OpenCV as Euclidean distances, and therefore was the valid metric. The results are summarized in Table 3. The table reports the accuracy of retrieving the correct individual in the rank 1 position.

As for LBPs and GFD, SIFT showed increasing accuracy when more training images were available per individual.

Table 3: Results using SIFT for feature extraction.

	# Images in Training Dataset		
	1	2	$n-1$
1-NN Euclidean	90.4%	96.0%	96.5%

4.4 Discussion

Using 493 images of 125 subjects of the IIT Delhi Ear Image Database, the recognition rates of the most descriptive feature vector of each of the three feature extraction techniques are shown in Table 4. SIFT gave the second highest accuracy in 5-NN, and the highest accuracy in 1-NN. We decided to use SIFT in our implementation of the iOS app since the ultimate goal of any biometric system is correct retrieval in the rank 1 position.

Table 4: Recognition rates (RR) of matches in the top-rank and top 5 ranks, for the three feature representations.

Methodology	RR (Top1)	RR (Top 5)
SIFT	96.5%	98.4%
FT	96.0%	99.2%
LBPs	95.5%	98.1%

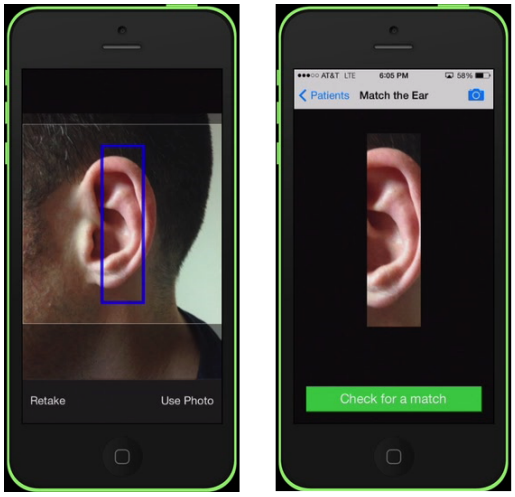

Figure 5: The interface for capturing an image of a patients ear. The top right camera icon (right) is available for recapturing an image if needed.

Figure 6: (left) shows the top ten ranks of a matching process, and (right) shows the medical history of the top matched record.

5 iOS APP

A prototype iOS app was developed to test the approach. Based on our experiments, we selected the SIFT algorithm for our implementation. The application has the following functionalities:

- Adding a new patient
- Viewing the information of an existing patient
- Editing the information of an existing patient
- Matching a visiting patient to database record

To acquire an image of the patient's ear, the application asks the health worker to align a bounding box with the subject's ear in order to perform ear detection. Figure 5 demonstrates the ear capture process. At this stage, the user has the choice of using the photo or re-taking it.

Once the photo has been captured, it is processed using the OpenCV library: cropped, downsampled, and converted to grayscale. SIFT features are then extracted from the captured image (Figure 7). At this stage, the medical practitioner has the option of retaking the image if it is blurry, or if the number of features detected is clearly much smaller than usual, for example two SIFT features.

The device's memory holds all feature vectors of patients that are currently in the database. There might be one or more feature vectors per individual depending on how many times the medical practitioner added new image descriptors to their record. Images are not stored on the device, only their descriptors are. This is done for privacy reasons, and for conserving the storage capacity on the mobile device. We are aware that a mobile device can be lost much more easily than say an on-site computer, and this raises security issues. We can envision a rudimentary approach where the app returns an ID, rather than full medical history, which can be used to retrieve the full medical record from a more secured system on-site. Built-in iOS hardware encryption can also be enabled. This approach can be further fortified; however, further encryption/obfuscation is beyond the current scope of the project.

Once a query is submitted, the SIFT feature vector of the input image is matched against the database using Euclidean. The top ten resulting matches are returned in the form of a ranked list (Figure 6). The medical practitioner can then select the patient record to display that patient's medical history (Figure 6). The process requires 5 clicks, and the matching occurs in less than five seconds for a database containing 838 image descriptors. Any on-site personnel can use this app after an hour of training.

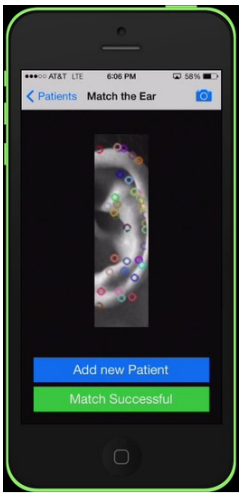

Figure 7: Screen capture of sample ear with SIFT points on application interface.

6 RESULTS: PILOT STUDY

A pilot study was performed in order to test the developed app in the same way the users would use it. Testing on a dataset collected in uniform laboratory settings is not sufficient because a controlled environment cannot be guaranteed in real future deployment. It is expected to note a drop in recognition percentages when using the mobile camera to capture images of individuals at different locations who are free to change pose between image captures, as opposed to a fixed capture laboratory setting used in the comparative study.

SIFT is scale and rotation invariant by design. The functionality of the bounding box reduces scale and in-plane rotation variations, and is used to reduce error propagation from automated ear detection. The remaining challenges that are not addressed in the prototype implementation are varying illumination and out-of-plane rotation.

A database was collected that contained 240 individuals: images gathered using our smartphone app for 115 individuals with 3 images each (345 images) plus the IIT dataset of 125 individuals with 3-6 images each (493 images). Thus, in total, there were 838 images (240 individuals) in the training database on the smartphone. A separate test set was used, which comprised 3 images per subject for 84 individuals who already had records in the database (yielding 252 test images total). The test images were excluded from training. The test images were captured on different days after the database was constructed.

Figure 8 summarizes the results. Although varying illumination and out-of-plane rotation were not addressed in the implementation of this app, 50% of

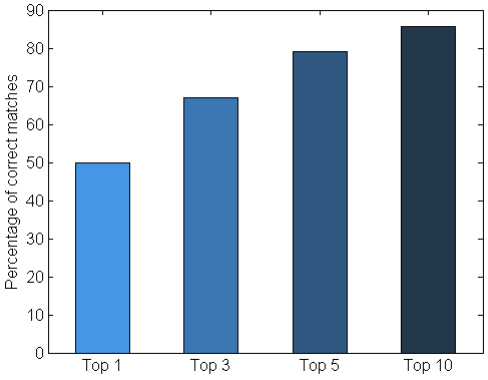

Figure 8: This graph shows the percentage of individuals (out of 84 test subjects) correctly matched to the top-rank record, to one of the top 3, top 5, and top 10 records.

the subjects matched their rank 1 position, whereas chance is 0.36%. 79% of the subjects matched one of the top 5 displayed ranks, whereas chance is 1.77%. 85.7% of the subjects matched one of the top 10 displayed ranks, whereas chance is 3.51%. It was interesting testing the app on twins; they matched themselves in the top rank, but matched each other next.

The pilot study suggests promising initial results for our proposed app. We expect percentages to improve when varying illumination and out-of-plane rotation are addressed. This would address the reason for the drop in recognition percentages between the two datasets. The future work section will address such next steps.

7 FUTURE WORK

Given the results of the pilot study, we plan three stages of future work in the order presented.

In order to select the suitable representation for the ear images, we performed a comparative study of three different feature extraction techniques on a controlled dataset, however the real world performance might be better for LBPs or GFD. We would like to implement LBP and GFD on the iOS app to have a better understanding of the real world performance of mobile ear biometrics.

In practice we found that LBPs and GFD are more computationally efficient and robust to varying illumination than SIFT features. On the other hand, we observed that SIFT attained higher retrieval accuracy in 1-NN (desired long-term behavior) when the illumination was controlled by a lab setting. This leads us to believe that using cascade LBPs, GFD, and SIFT based classifiers, would improve robustness of our system. Also, using the flash on the smartphone could be used to further improve the accuracy of our system mimicing standard lighting conditions.

Further information like sex or rough age can be used to distinguish the patient identity. For example, we would like to integrate a pre-filtration feature in the app based on sex. Only records matching the sex entered by the medical practitioner would be displayed in the ranked list. The medical practitioner can then perform manual post-filtration by approximate age, or approximate name spelling to match an individual within the displayed top 10 ranks.

Although 1-NN $\sim$ 100% accuracy is the target for any biometric based application, even a $\sim$ 100% 10-NN accuracy would greatly contribute to providing higher quality healthcare in such on-site clinics at this stage. This is our short-term goal. Having a medical practitioner find an individual's record among 10 ranked options, is much better than having nearly no chance of getting to a patient's medical record. We would like to further investigate usability metrics like throughput rates and additional precision metrics like false positive identification-error rate for unenrolled individuals [Biometrics Metrics Report v3.0, 2012]. All testing has been done on adults, however in on-site medical clinics, vaccination of infants is one of the major requirements. Therefore, future work also includes performing a longitudinal study on infants under the age of three whose ears will be developing over time. This would follow the three stages of improving the app performance on adult recognition.

8 CONCLUSION

We proposed a formulation, developed a prototype, and conducted preliminary testing of an iOS application to identify individuals based on ear biometrics. The application allows a medical practitioner to take a photo of a patients ear, and return the top ten matches within a database of medical data contained locally on the phone. The application is a non-invasive, easy to use, tolerant to capture rotation and scale, and requires the use of relatively cheap and increasingly ubiquitous device, the smartphone. In our pilot study, the prototype app was able to retrieve the correctly matching record ranked within the top 5, 79% of the time. Although this percentage is currently low for a real application deployment, this is work in progress that lays the foundation for future work described in the previous section, and for a feasibile application deployment we believe.

We hope that this work will serve as a catalyst to solve patient identification problems at on-site med-

ical clinics in less developed countries, and have a positive impact on global health. Although the main target of the app is identifying subjects for the purpose of cataloging their medical data in field settings, it would also be useful for on-site identification of casualties complicated by facial injury and lack of identifying documents.

ACKNOWLEDGMENTS

We would like to thank the Biometrics Research Laboratory at IIT Delhi for providing us with the IIT Delhi Ear Image Database. We would also like to thank Fatih Cakir for bringing together the public health and computer science teams.

REFERENCES

Abate, A., Nappi, M., Riccio, D., and Andricciardi, S. (2006). Ear recognition by means of a rotation invariant descriptor. *Pattern Recognition, ICPR. 18th International Conference on*, 4:437–440.

Abaza, A., Ross, A., Hebert, C., Harrison, M. F., and Nixon, M. S. (2013). A survey on ear biometrics. *ACM Computing Surveys (CSUR) Journal*, 45(2):22.

Abdel-Mottaleb, M. and Zhou, J. (2005). Human ear recognition from face profile images. *Advances in biometrics*, pages 786–792.

Azfar, R. S., Weinberg, J. L., Cavric, G., Lee-Keltner, I. A., Bilker, W. B., Gelfand, J. M., and Kovarik, C. L. (2011). HIV-positive patients in botswana state that mobile teledermatology is an acceptable method for receiving dermatology care. *Journal of telemedicine and telecare*, 17(6):338–340.

Biometrics Metrics Report v3.0 (2012). Prepared for: U.S. Military Academy (USMA) - West Point. http://www.usma.edu/ietd/docs/BiometricsMetricsReport.pdf.

Biometrics Research Laboratory (2013). IIT Delhi Ear Database. http://www4.comp.polyu.edu.hk/~csajaykr/IITD/Database_Ear.htm.

Boodoo-Jahangeer, N. B. and Baichoo, S. (2013). LBP-based ear recognition. *Bioinformatics and Bioengineering (BIBE), IEEE 13th International Conference on*, pages 1–4.

Bradski, G. (2000). Dr. Dobb's Journal of Software Tools.

Chang, K., Bowyer, K., Sarkar, S., and Victor, B. (2003). Comparison and combination of ear and face images in appearance-based biometrics. *Pattern Analysis and Machine Intelligence, IEEE Transactions on*, 25(9):1160–1165.

Cummings, A., Nixon, M., and Carter, J. (2010). A novel ray analogy for enrollment of ear biometrics. *Biometrics: Theory Applications and Systems (BTAS), Fourth IEEE International Conference on*, pages 1–6.

Delac, K. and Grgic, M. (2004). A survey of biometric recognition methods. *Electronics in Marine, 2004. Proceedings Elmar 2004. 46th International Symposium*, pages 184–193.

Fahmi, A., Kodirov, E., Choi, D., Lee, G., M. F. Azli A., and Sayeed, S. (2012). Implicit authentication based on ear shape biometrics using smartphone camera during a call. *Systems, Man, and Cybernetics (SMC), IEEE International Conference on*, pages 2272–2276.

Goode, A. (2014). Bring your own finger–how mobile is bringing biometrics to consumers. *Biometric Technology Today*, 2014(5):5–9.

Iannarelli, A. (1989). Ear identification, forensic identification series, fremont. *Paramont Publishing Company, Calif, ISBN*, 10:0962317802.

Kisku, D. R., Mehrota, H., Gupta, P., and Sing, J. K. (2009). SIFT-based ear recognition by fusion of detected keypoints from color similarity slice regions. *Advances in Computational Tools for Engineering Applications, 2009. ACTEA'09. International Conference on*, pages 380–385.

Kumar, A. and Wu, C. (2012). Automated human identification using ear imaging. *Pattern Recognition*, 45(3):956–968.

Kumar, M. (2014). Hanseatic institute of technology. cell phone-based intelligent biometrics. http://www.appropedia.org/Cell_phone-based_intelligent_biometrics.

Kwapisz, J. R., Weiss, G. M., and Moore, S. A. (2010). Cell phone-based biometric identification. *Biometrics: Theory Applications and Systems (BTAS), Fourth IEEE International Conference on*, pages 1–7.

Lowe, D. (1999). Object recognition from local scale-invariant features. *Computer vision. The proceedings of the seventh IEEE international conference on*, 2:1150–1157.

Mäenpää, T., Ojala, T., Pietikäinen, M., and Soriano, M. (2000). Robust texture classification by subsets of local binary patterns. *Pattern Recognition, 2000. Proceedings. 15th International Conference on*, 3:935–938.

Ojala, T., Pietikainen, M., and Harwood, D. (1996). A comparative study of texture measures with classification based on feature distributions. *Pattern Recognition*, 29(1):51–59.

Takala, V., Ahonen, T., and Pietikäinen, M. (2005). Block-based methods for image retrieval using local binary patterns. *Image Analysis*, pages 882–891.

Vedaldi, A. and Fulkerson, B. (2008). VLFeat: An open and portable library of computer vision algorithms. http://www.vlfeat.org/.

Wang, Y., Mu, Z., and Zeng, H. (2008). Block-based and multi-resolution methods for ear recognition using wavelet transform and uniform local binary patterns. *Pattern Recognition, ICPR. 19th International Conference on*, pages 1–4.

Zhang, D. and Lu, G. (2002). Shape-based image retrieval using generic fourier descriptor. *Signal Processing: Image Communication*, 17(10):825–848.